Heliyon 8 (2022) e11089

Contents lists available at ScienceDirect

Heliyon

journal homepage: www.cell.com/heliyon

Research article

Isolation, partial characterization and *in vitro* digestion of starch from *Ariopsis peltata* and *Lagenandra toxicaria* tuber

B. Akarsha, Karunya Shetty, G. Krishnakumar *

Department of Applied Botany, Mangalore University, Mangalagangothri, 574199, India

GRAPHICAL ABSTRACT

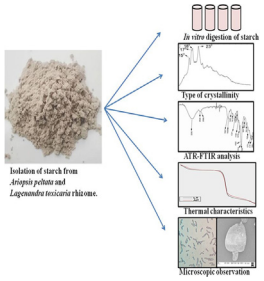

ARTICLE INFO

Keywords:
Amylose
Crystallinity
Gelatinization
Rapidly digestible starch
Thermogravimetric analysis
X-ray diffraction

ABSTRACT

The starch from two aroid tuber *viz*. *Ariopsis peltata* and *Lagenandra toxicaria* were isolated and evaluated for their morphological, physical and chemical properties. The tubers of these plants are used as food and medicine by the indigenous communities. The starch yield from *A. peltata* tuber was 25 ± 1.7% with an amylose content of 10 ± 0.9%, while the tuber of *L. toxicaria* contained 28 ± 6.5% starch with 15 ± 0.5% of apparent amylose in it. The starch isolated from both the tubers was highly pure (99%) starch exhibiting an A-type X-ray diffraction pattern. The starch granules of *L. toxicaria* were of various shapes and exhibited a smooth surface without any cleft or break. While the starch granules of *A. peltata* were spherical with smooth surface, as well as rough surface. The breaks and clefts were apparent on the rough-surfaced granules. The gelatinization temperature range for *A. peltata* and *L. toxicaria* starch is approximately 23 °C and 19 °C respectively. *A. peltata* starch showed higher thermal stability compared to *L. toxicaria* starch and either of the starch was rapidly digestible as evident from *in vitro* digestion study. The physicochemical properties of both the starches render them stable to withstand extreme processing. Besides they also mimic simple sugar in digestibility. So it can be utilized as a substitute for simple sugars in brewing and pharmaceutical industries.

1. Introduction

Starch is the basic source of nutrition and energy for plants and animals, synthesized in plastids and exists as semicrystalline granules. It is the second most important biopolymer consisting of branched amylopectin and linear amylose units (Betancur et al., 2001; Kuttigounder et al., 2011; Singh et al., 2007). Each plant starch has diverse physicochemical properties and is a storage product found in leaf chloroplast or amyloplast of seeds, roots, tuber, etc (Ochubiojo and Rodrigues 2012). Most of these storage organs are used as food by humans (Jobling, 2004).

This article is a part of the "Unconventional sources of food and food ingredients" Special issue.

* Corresponding author.
E-mail address: kkgtaxo13@gmail.com (G. Krishnakumar).

https://doi.org/10.1016/j.heliyon.2022.e11089
Received 27 October 2021; Received in revised form 14 February 2022; Accepted 10 October 2022

The industrial application of starch depends on the availability and physicochemical characteristics of starch (Pascoal et al., 2013). Starch finds application in the paper (for enhancing paper strength and printing properties), pharmaceutical (as drug filler), packaging (as a binder), textile (sizing of fine fabrics), cosmetic, and food industry. In the food industry, it is used as a food additive to regulate consistency and texture, withstand the breakdown of gel during processing and enhance the shelf-life of end products (Falade and Okafor, 2013). Most of the naturally occurring starches have limited application in the food industry owing to their poor process tolerance, high retrogradation, weak shear and heat resistance, higher viscosity and thermal decomposition. Also, cooked starches form a weak, cohesive and rubbery paste (Alcázar-Alay and Meireles, 2015; Eliasson and Gudmundsson, 1996). Because of these limitations of conventionally available starch, investigators are looking for new sources of starch with better physicochemical properties. The starch from maize, rice, wheat, potato and cassava is widely used to produce commercial starches. In addition to these, starch is isolated from non-conventional sources such as tubers of aroid plants like *Alocasia macrorrhiza, Amorphophallus campanulatus, Colocasia esculenta, Cyrtosperma merkusii* and *Xanthosoma sagittifolium* (Zhu, 2016).

Ariopsis peltata (AP) and *Lagenandra toxicaria* (LT) belong to the family Araceae. AP is an endemic, lithophytic, perennial herb with tubers. LT is commonly seen in marshy regions of south India. It's leaves are used as food and the tubers are used by traditional healers to treat bilious complaints, renal and cardiac ailments. The plant is recognized to be diuretic, carminative and used as a tonic (Selvakumari, 2014). Most of the Araceae members are rich in the storage protein lectin (Van et al., 1995), which is used in anticancer therapeutics as it can bind to the cancer cell membranes and/or receptors causing cell apoptosis (De Mejia and Prisecaru 2005). Besides, there is no information available on the physicochemical properties, crystallinity and in vitro digestibility of starch from these two plants.

The present study is to assess the physicochemical properties of the starch of these two lesser-known plant tubers. We determined the purity of the isolated starch, apparent amylose content, physicochemical properties (swelling factor and pasting properties), crystalline structure and *in vitro* starch digestibility.

2. Material and methods

2.1. Reagents

Amylose from potato (CAS no. 9005-82-7) and α-amylase from porcine pancreas (A3176-500ku, EC.No.232-565-6) were obtained from SIGMA Aldrich chemical co. India. Sodium metabisulphite from Nice chemicals, Kerala, India. All the other chemicals used were of analytical grade.

2.2. Plant collection and isolation of starch.

AP tubers were collected from Charmadi ghat (an integral part of the Western Ghats), Dakshina Kannada, Karnataka, India (13°04′35″ N, 75°27′06″ E). While LT tubers were collected from Markanja village of Sullia, Dakshina Kannada, Karnataka, India (12°34′38.7″ N, 75°.29′54.8″ E). The herbaria (AK 08, AK 09) of both the plants were prepared and deposited in the Department of Applied Botany, Mangalore University. Collected tubers were washed, chopped and shade dried. The dried samples were powdered and starch was isolated using sodium metabisulphite following the method of Chandra et al. (2016). The isolated starch was dried and weighed, the yield from each sample was calculated (Eq. (1)) and starch content was determined using the anthrone method (Sadashivam and Manickam 2008).

$$\text{Yield } (\%) = \frac{Ws}{W} \times 100 \quad (1)$$

Here, Ws is the weight of the starch and W is weight of the sample.

2.3. Physicochemical analysis of starch

2.3.1. Apparent amylose content and pH of the starch.

10 ml of 1:9 (v/v) mixture of Ethanol: 1N NaOH was added to 100 mg of powdered starch sample and incubated overnight, after which, the volume was made up to 100 ml using distilled water. Further, 2.5 ml of this extract was diluted with 20 ml of distilled water. To this, three drops of phenolphthalein indicator was added followed by the addition of 0.1N HCl dropwise until the pink colour disappears. 1.0 ml of Iodine solution (0.2%) was added to this mixture and the volume was made up to 50 ml using distilled water. Absorbance was measured at 590 nm. Amylose content was calculated using the potato amylose standard curve (Sadashivam and Manickam 2008). The pH of the starch was measured using a Systronics digital pH meter.

2.3.2. Water holding capacity

One gram of starch was suspended in 15 ml of distilled water and stirred for 1 h. Free water was drained from the wet starch. After 10 min, the wet starch was weighed and the result was given as percent on a dry weight basis (Eq. (2)) (Deepika et al., 2013a).

$$\text{Water holding capacity } (\%) = \frac{Ws}{Ds} \times 100 \quad (2)$$

Here, Ws is the weight of the wet starch and Ds is the weight of the dry starch.

2.3.3. Paste clarity

A 2% starch suspension (w/v) was prepared in distilled water and incubated for 30 min in a boiling water bath and stirred thoroughly after every 5 min. Samples were then stored at 4 °C for 5 days. The transmittance of the stored sample was recorded at 640 nm after every 24 h using a spectrophotometer against water as a blank (Ochubiojo and Rodrigues 2012; Perera and Hoover 1999).

2.3.4. Swelling power and solubility

The swelling property and solubility of the starch were observed at temperatures of 60 °C, 70 °C, 80 °C and 90 °C. Slurry of the starch was prepared by dispersing starch in distilled water (1% w/v). The resulting slurries were heated at 60 °C, 70 °C, 80 °C and 90 °C in a waterbath for 1 min with continuous stirring. Then the slurries were cooled to room temperature and centrifuged at 3000 rpm for 15 min. The wet starch pellet was weighed (Ws) while the supernatants were decanted to a preweighed petridish and evaporated until dry at 110 °C. The weight of the residue (W_2) was determined after drying. The percentage of solubility and swelling of the starch was calculated using the formula (Eqs. (3) and (4)) given by Zhang et al. (2017) and Chel-Guerrero et al. (2016).

$$\text{Swelling Power } (g/g) = \frac{Ws}{(100 - \%\ \text{Solubility}) \times S} \times 100 \quad (3)$$

$$\%\ \text{Solubility} = \frac{\text{Weight of soluble starch}}{S} \times 100 \quad (4)$$

Here, Ws is the weight of wet starch (g) and S weight of starch on a dry weight basis (g).

2.3.5. Morphology of the starch granules

The shape and morphology of the starch granules were examined using a field emission scanning electron microscope (FESEM) Carl Zeiss 03–81 Germany. The granules were sprinkled on the double-sided adhesive tape mounted on a metal stub, followed by gold sputtering. The image was obtained under 5 kV (Chen et al., 2018; Xia et al., 2015). The granule size was calculated using ocular micrometry fitted to an optical microscope (Olympus CH20iBIMF) under 400x magnification (Lobo and Gulimane, 2015; Zhang et al., 2018). The images of the granules were captured using Canon power shot SX400.

2.3.6. Type of crystallinity

The starch samples were equilibrated with a saturated solution of KCl for one week to adjust their moisture content to approximately 20%. The crystallographic pattern of AP and LT starch were determined using XRD [*Rigaku miniflex* 600 with CuKα radiation (λ = 0.15406 nm)] under the following conditions: region of scanning angle 2θ ranged from 3° to 80° for both the samples, operated at an emission current 15 mA and an accelerated voltage of 40 kV with a scanning speed of 1° per minute. The percentage of crystallinity was measured in Origin pro 9.0 software using Eq. (5) (Malumba et al., 2017; Zhang et al., 2011).

$$\text{Crystalline } \% = \frac{Ac}{Ac + Aa} \times 100 \quad (5)$$

Here, Aa is the amorphous area, while Ac is the total area of crystalline peaks and Ac + Aa is the total area.

2.3.7. ATR-FTIR spectroscopy

The carbohydrate nature of the isolated starch sample was examined using ATR-FTIR. The spectrum of the starch sample was recorded at 300 to 4000 cm^{-1} wavenumber range at room temperature (Ashwar et al., 2017; Zeng et al., 2014).

2.3.8. Thermal characteristics

The gelatinization temperature, gelatinization enthalpy and thermal stability were analyzed using a Universal thermal analyzer (Sl. no. 0600-1399 SDT Q600 V20.9 Build 20). The instrument is equipped to carry out both Differential Scanning Calorimeters (DSC) and Thermogravimetric analysis (TGA) simultaneously. About 4–8 mg of starch samples were heated to 25 °C to 500 °C under nitrogen gas (100 ml/min) with a scan rate of 10° C/min. The temperature at which gelatinization begins is onset temperature (T_0) while the peak temperature (T_p) is the temperature at which gelatinization is maximum and the temperature at which the gelatinization process terminates is referred to as conclusion temperature (T_c). The enthalpy change of gelatinization (ΔH) was recorded and the gelatinization temperature range (T_c-T_o) was calculated (Malumba et al., 2017; Kouser et al., 2020). The thermal stability of isolated starch was determined from TGA data (Malumba et al., 2017; Abera et al., 2019; Kouser et al., 2020).

2.3.9. Starch hydrolysis

Isolated starch was hydrolyzed by the porcine pancreatic α-amylase (PPA) enzyme following Zhu et al. (2018). 10 mg of the isolated starch was separately subjected to enzyme hydrolysis with 2 ml of PPA enzyme solution (contains 50 U PPA, 25 mM NaCl, 5 mM $CaCl_2$, 0.02% NaN_3, in 0.1 M sodium phosphate buffer pH 6.9) for 1, 2, 4, 8, 12, 24 and 48 h at 37 °C in a thermostat water bath with continuous shaking. After the hydrolysis, the mixture was subjected to centrifugation at 5000 g for 5 min. The recovered supernatant was used for the soluble carbohydrate analysis using the Anthrone method with glucose as standard. The degree of hydrolysis of the starch was calculated using Eq. (6).

$$\text{Hydrolysis degree } (\%) = \frac{\text{Quantity of soluble carbohydrates} \times 0.9}{\text{Initial weight of starch}} \times 100 \quad (6)$$

2.4. Statistical analysis

All the experiments were carried out in triplicates and the results are presented as mean ± SD. The data were analyzed and compared using the student t-test (PRISM Graphpad, version 5.0; Graphpad Software Inc., San Diego, CA).

3. Results and discussion

3.1. Yield and pH of the starch samples.

Both the isolated starch was light brown and had smooth texture. The starch yield and purity in AP was 24.72 ± 1.74 and 99.26 ± 8.93%, respectively, while starch yield and purity in LT was 28.33 ± 6.51 and 99.65 ± 2.44% respectively. The members of Araceae are reported to have a starch yield ranging from 22% to 40% (Deepika et al., 2013a). The pH values of the starches are given in Table 1. The pH of LT was neutral while that of AP was slightly acidic.

3.2. Apparent amylose

The apparent amylose content in LT and AP starch were 15.12 ± 0.47% and 10.27 ± 0.92% respectively (Table 1). The apparent amylose in most of the aroid tubers ranges from 13 to 28% (Table 2). Amylose content determines the physicochemical property of the starch (Zhang et al., 2017). The lower percentage of amylose implies higher proportions of amylopectin. The percentage composition of amylose and amylopectin determines the granule size and shape (Singh et al., 2016). Further, the gel textural and pasting property of starch is determined by the amylose content in it while amylopectin contributes to the firmness.

3.3. Water holding capacity.

The water holding capacity of both the isolated starch is given in Table 1. AP and LT starch show 357.86 ± 13.14% and 314.18 ± 5.64% of water holding capacity respectively. The lower water holding capacity of LT starch may be due to the formation of a larger proportion of hydrogen bonds within the starch than with that of water (Deepika et al., 2013a).

3.4. Paste clarity

The percentage transmittance increased in both samples (Figure 1). On the fifth day, LT showed 71.1 ± 1.82% and AP showed 81.97 ± 0.55% of transmittance. The paste clarity is related to the state of dispersion and the retrogradation tendency of the starch. It relies on the granule size, structure, paste concentration and pH of the starch. Further, the percentage of light transmittance of the starch paste is closely related to the swelling and solubility of the starch. Increased light transmittance indicates a higher swelling power of the starch granules (Ashwar et al., 2017; Deepika et al., 2013a, 2013b). The higher paste clarity of both the samples in this study may be due to the smaller granule size of the starches.

3.5. Swelling properties and solubility of starch

The swelling power and solubility percentage of LT and AP starch granules at different temperatures ranging from 60 °C to 90 °C is represented in Table 3. From 60 °C to 70 °C slight increase in the swelling property of starch was recorded, but from 70 °C to 90 °C starch samples showed a sudden increase in both swelling properties and solubility. The swelling property, water holding capacity and solubility is related directly to an increase in temperature. The presence of a non-covalent bond between starch molecules favors the swelling and water holding capacity of starch (Ubalua, 2007). Increasing the temperature of the

Table 1. Physicochemical and morphological characteristics of starch isolated from aroid tubers.

	Ariopsis peltata	*Lagenandra toxicaria*
Yield (%)	24.72 ± 1.74[a]	28.33 ± 6.51[a]
Starch content (%)	99.26 ± 8.93[a]	99.65 ± 2.44[a]
pH	5.8 ± 0.15[a]	6.5 ± 0.36[b]
Water holding capacity (%)	357.86 ± 13.14[a]	314.18 ± 5.64[b]
Mean of granule size (μm)	13.77 ± 4.83[a]	21.23 ± 6.35[a]
Granule size range (μm)	5–25	10–37.5
Amylose (%)	10.27 ± 0.92[a]	15.12 ± 0.47[b]

All the results are presented as mean ± SD. The columns with different superscript are significantly different ($p < 0.05$).

Table 2. Physicochemical properties of some Aroid starch.

Plant	Amylose content (%)	Granule size (μm)	Crystalline type	Starch Yield %	Reference
Colocasia esculenta varieties	14–28	5–10	A	6–14	Deepika et al. (2013a, 2013b) Zeng et al. (2014)
Xanthosoma sagittifolium	18	2.1–2.28	A	NA	Saikia and Konwar (2012)
Xanthosoma caracu	13	1.25–2.21	A	NA	Saikia and Konwar (2012)
Amorphophallus paeoniifolius	13	5–12	A	NA	Saikia and Konwar (2012)
Alocasia indica Linn.	NA	4.77	NA	NA	Lodha and Nemade (2012)

**NA* – Not Available.

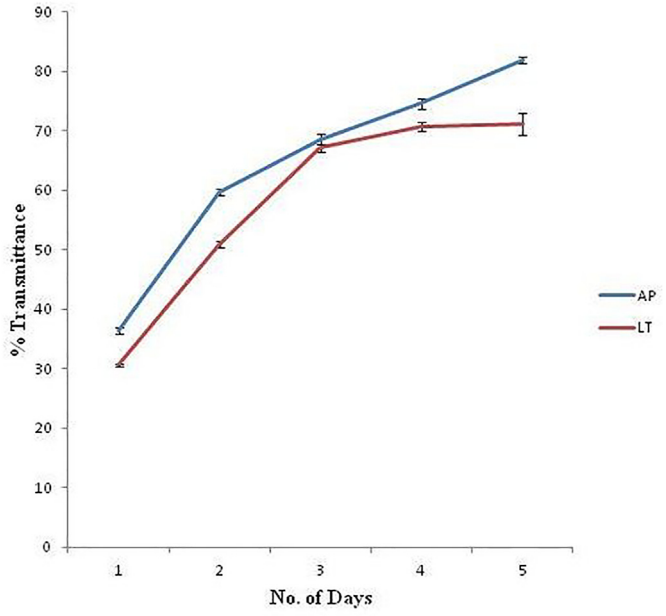

Figure 1. Paste clarity of AP and LT starch.

Table 3. Swelling power and solubility of the isolated starch.

Temperature	Solubility (%)		Swelling power (g/g)	
	Ariopsis peltata	*Lagenandra toxicaria*	*Ariopsis peltata*	*Lagenandra toxicaria*
60 °C	8.8 ± 0.4^{a}	4.53 ± 0.42^{b}	5.20 ± 0.03^{a}	4.74 ± 0.09^{b}
70 °C	14.06 ± 0.31^{a}	9.93 ± 0.70^{b}	5.73 ± 0.10^{a}	5.27 ± 0.04^{b}
80 °C	31.47 ± 0.95^{a}	23.67 ± 0.58^{b}	12.93 ± 0.17^{a}	10.48 ± 0.17^{b}
90 °C	38.2 ± 0.92^{a}	29.27 ± 0.90^{b}	18.77 ± 0.34^{a}	14.06 ± 0.12^{b}

All the results are presented as mean ± SD. The data were analyzed and compared using student t-test. The columns with different superscript are significantly different ($p < 0.05$).

starch suspension causes hydration of the structure due to rupture of the intermolecular bridges in amorphous zones, thereby increasing the swelling property of the starch granules. Furthermore, the swelling capacity of starch is positively correlated with the amylopectin content and negatively correlated with amylose. Therefore, higher amylose content inhibits swelling. Along with that, other factors also affect the swelling property of the granules, like small-sized granules swell more compared to larger sized granules at a higher temperature. The starch granules that are highly associated with strong and extensive micellar structure display relatively lower swelling and solubility (Singh et al., 2003). Furthermore, starch that contains amylose – lipid complexes also exhibits restriction on swelling and solubility (Alcázar-Alay and Meireles, 2015; Wang et al., 2017).

3.6. Crystalline structure of starch

AP and LT starch have 18.08% and 20.44% of crystallinity respectively. The crystallinity of both the starch granules was lower than that of *Amorphophallus paeoniifolius* (33%) and rice (34%) starch (Sukhija et al., 2016; Yang et al., 2019). Both the starch showed an A-type crystalline structure with characteristic reflection at about 15°, 23° 2θ and an unresolved doublet at 17° and 18° 2θ as observed in the diffractogram (Figure 2). The diffractograms of most of the aroid starches are similar to this (Lertphanich et al., 2013; Saikia and Konwar, 2012; Zeng et al., 2014).

The diffraction pattern of starch is related to the chain length and distribution of amylopectin. Based on this, there are three types of starches A, B, and C (Lertphanich et al., 2013). The A-type starches exhibit strong reflection at 15°, 23° and an unresolved doublet at 17° and 18°. B-type crystalline starches exhibit characteristic reflection at 5.6°, 15°, 17°, 22° and 23° and C-type crystalline starches exhibit both A and B diffractograms and will be further classified into CA-, CB-, and CC-type

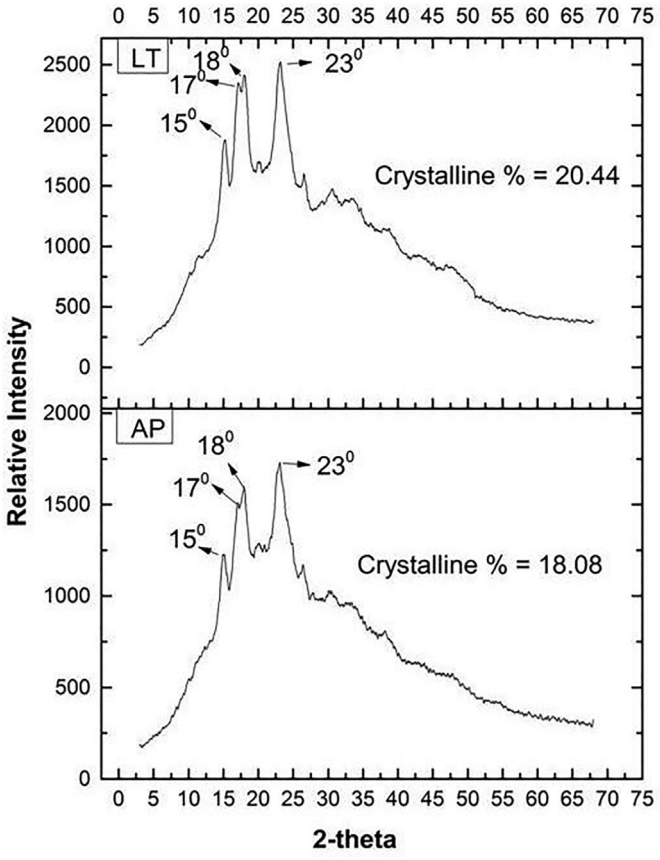

Figure 2. XRD pattern of LT and AP starch granules.

based on their resemblance to A- and B-type or between the two types, respectively. Earlier studies suggest that starch with low amylose content shows an A-type XRD pattern (Lertphanich et al., 2013; Wani et al., 2015; Riley et al., 2004; Padmanabhan and Lonsane, 1992). This is further corroborated by this study.

3.7. Chemical vibration authentication using ATR-FTIR

The absorption of infrared energy depends on the variation in the crystal structure, difference in helical structure and chain conformation of the starch (Ashwar et al., 2017). Infrared absorption spectra showed (Figure 3) three characteristic vibrations between 926 cm^{-1} and 1150 cm^{-1}, which represents the C–O bond stretching. Peaks at 999 cm^{-1}, 1014 cm^{-1}, 1022 cm^{-1}, 1076 cm^{-1} and 1150 cm^{-1} refer to anhydroglucose ring C–O stretch of C–O–H in starch. The vibration at 1647 cm^{-1} represents strongly bound water present in the starch (Deepika et al., 2013a, 2013b; Zeng et al., 2014). The absorption band at 2928 cm^{-1} and 2929 cm^{-1} is contributed by C–H stretching vibration. Absorption bands in the region of 1365–1410 cm^{-1} correspond to the C–H bending vibrations. The broadband stretching vibration at 3290 cm^{-1} indicates the presence of hydroxyl group (O–H). In this study, it is clear that there are no major differences in the isolated starches from two different plant tubers as is seen in Figure 3.

3.8. Morphology of the starch granule

Morphology and granule size of starch vary with plant genotype. It also depends on the biochemistry of the chloroplast or amyloplast, as well as the physiology of the plant (Liu et al., 2018; Pfister and Zeeman 2016). The granule size varied from 10 to 37.5 μm in LT starch and 5–25 μm in starch isolated from AP. The mean values of the granule size are given in Table 1. The average size of the starch granules of most of the aroid tubers ranges from 1 to 10 μm (Table 2). The FESEM and optical microscopic images of the LT starch show (Figures 4 and 5) a smooth surface without any cleft and break. The shape of the starch granule varies, some were dumbbell-shaped, but most of them were curved. While spherical shaped granules (Figures 4 and 5) with both smooth and rough surfaces were seen in AP starch. Breaks and clefts were found in AP starch granules with a rough surface. Cracks may be due to low particle integrity stemming from the defective packing of amylopectin double-helical molecules. This was also found in transgenically modified potatoes (Blennow et al., 2003) and pulse starches (Ambigaipalan et al., 2011).

3.9. Thermal property

Gelatinization results due to the disruption of molecular arrangement within the starch granule. This manifests as irreversible changes in properties such as granular swelling, native crystallite melting, loss of birefringence and starch solubilization. Gelatinization temperature varies based on the crystalline nature of the starch. Also, gelatinization temperature directly relates to the degree of arrangement of molecules in starch granules (Abera et al., 2019). Reports suggest that starches with A-type crystallinity show more gelatinization temperature compared to starches with B-type crystallinity. Also, starch with higher granule size and varied shape exhibit higher gelatinization temperature (Wang et al., 2018). LT and AP showed higher gelatinization temperature and enthalpy (Figure 6 & Table 4) of 14.22 J/g and 19.52 J/g respectively. This is greater than the corn (12.3 J/g) and wheat (10.7 J/g) starches (Jane et al., 1999; Singh et al., 2003). More enthalpy represents the quantity and quality of crystallinity and also indicates the loss of molecular arrangement of starch granules (Jane et al., 1999). The higher change in enthalpy (ΔH) in AP and LT starch might represent the formation of longer and more double helices by the amylopectin external chains (Zhang et al., 2017). Thermogravimetric analysis (TGA) reveals the thermal stability of starch samples (Figure 7). The weight

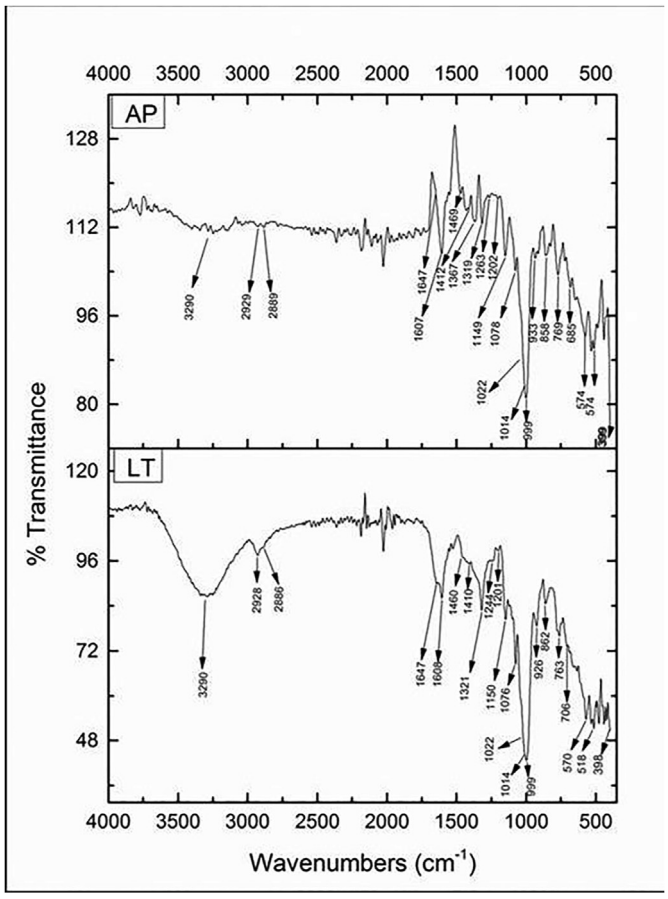

Figure 3. ATR-FTIR spectra of LT and AP starch.

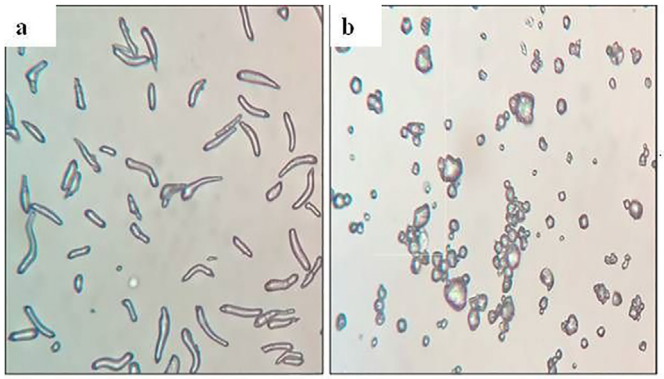

Figure 4. Optical microscopy images of starch granules as observed under 400x magnification. a) *Lagenandra toxicaria.* b) *Ariopsis peltata.*

loss occurred in three sections. During the first section, from 25 °C to 240 °C about 13.52% and 13.63% of weight loss was observed for LT & AP starch respectively. The stability of either of the starch was comparably same during this section. While in the second section of 240 °C–320 °C, weight loss of LT starch was more (71%) compared to AP starch (68%). This suggests that AP starch is thermally more stable than LT starch.

3.10. In vitro digestion

PPA hydrolysis study imitates the hydrolysis in the small intestine and blood glucose level response to starch. The hydrolysis rate of the AP and LT starch is given in Figure 8. The hydrolysis rate increased drastically for

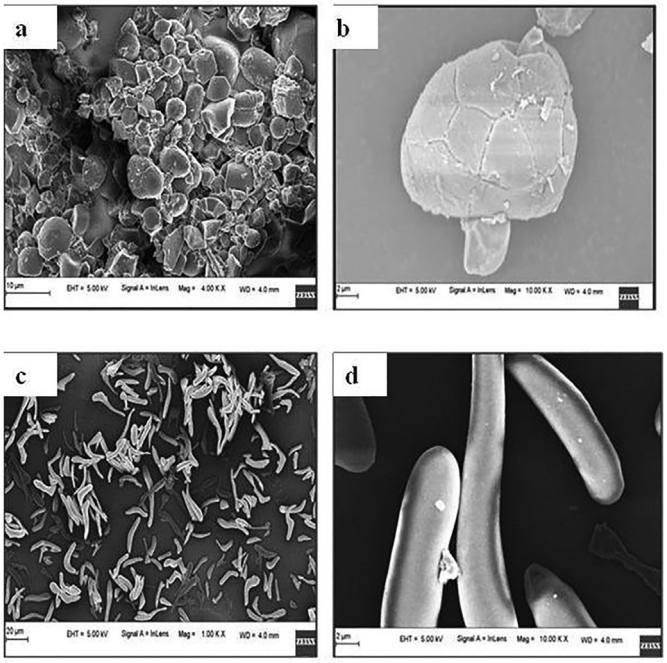

Figure 5. FESEM images of starch granules under various magnification. a) Cluster of AP starch. . b) Single AP starch grain. c) Cluster of LT starch. d) LT starch grains.

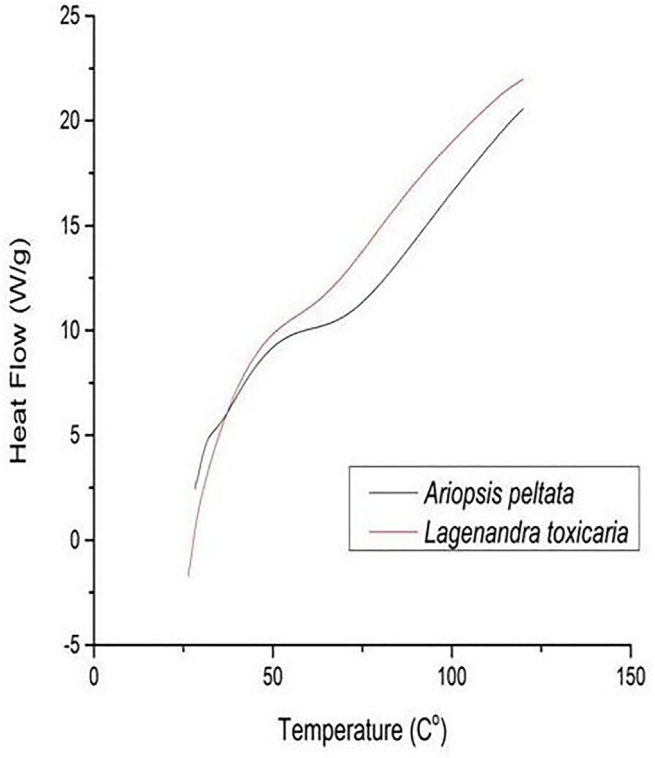

Figure 6. DSC thermogram of the *Lagenandra toxicaria* and *Ariopsis peltata* starch.

LT starch as compared to the starch of AP in the first hour of reaction. After 1 h, the hydrolysis rate for AP starch increased as compared to LT starch. Both samples showed a great extent of hydrolysis i.e. 43.48 ± 2.31% for LT starch and 56.73 ± 2.73% for AP starch up to 12 h, after which the hydrolysis rate reached a plateau. The previous report suggests that A-type granules present in normal maize, wheat and rice starches show a much faster rate of hydrolysis than B-type (potato) starch due to a greater extent of structural defects in granules (Jane, 2006; Riley et al., 2004). The digestion of starch also depends on the amylose and amylopectin content (Hoover, 2001). The hydrolysis rate increases with decreased amylose content, for example, the hydrolysis rate of Cassava starch is faster than potato starch since it has less amylose content (Padmanabhan and Lonsane, 1992). Amylose restricts the digestion of starch. The susceptibility of the starch to amylase is dependent on granule size, morphology and porosity. Starch with a larger granule size and low relative surface area will be hydrolyzed slowly by the enzymes compared to the starch with a smaller granule size. Also, pores and channels in the granules will increase the susceptibility of the granules to the amylase enzyme (Zeng et al., 2014; Zhu et al., 2018). The starch of AP has a smaller granule size with cracks on the surface of granules and lower amylose content as compared to the LT starch (Table 1). Hence AP starch sample might be more susceptible to enzyme hydrolysis making it readily digestible.

Table 4. Thermal characteristics of starch isolated from aroid tubers.

Temperature	*Ariopsis peltata*	*Lagenandra toxicaria*
T_o (onset)	49.19 ± 0.25[a]	47.73 ± 0.15[b]
T_p (peak)	54.71 ± 0.02[a]	52.37 ± 0.21[b]
T_c (conclusion)	72.29 ± 0.05[a]	66.8 ± 0.1[b]
T_c-T_o (gelatinization temperature range)	23.09 ± 0.25[a]	19.07 ± 0.05[b]
Enthalpy change	19.52 ± 0.04[a]	14.22 ± 0.12[b]

All the results are presented as mean ± SD. The columns with different superscript are significantly different ($p < 0.05$).

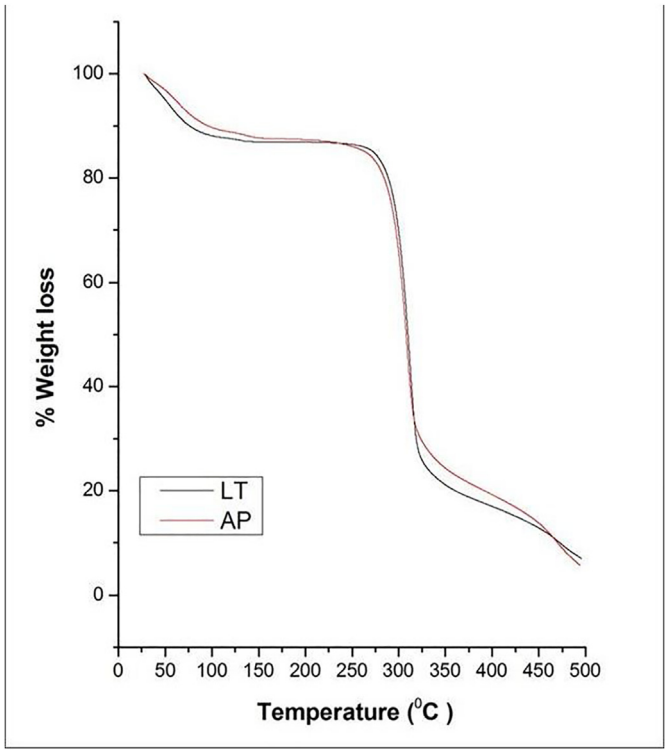

Figure 7. Thermogravimetric analysis (TGA) of the *Lagenandra toxicaria* and *Ariopsis peltata* starch.

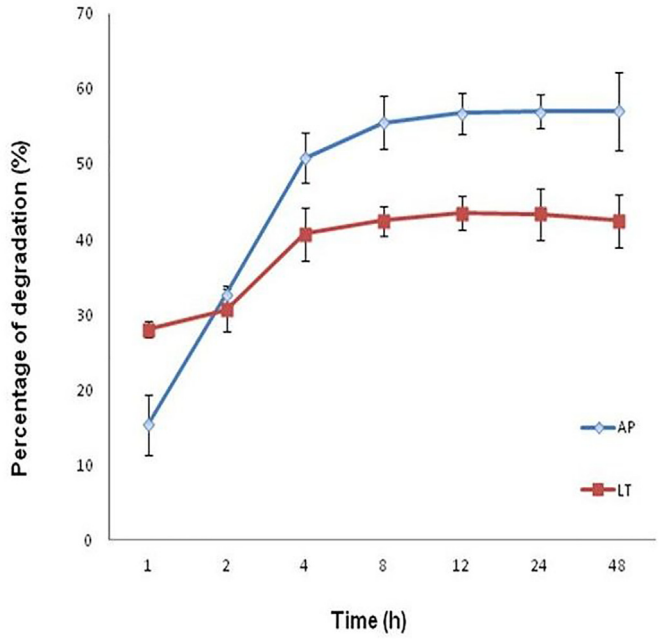

Figure 8. Percentage of degradation of the *Lagenandra toxicaria* and *Ariopsis peltata* starch hydrolysed by PPA enzyme.

4. Conclusion

A good amount of starch was obtained in the tubers of both the plants. The isolated starches showed differences in morphology, physicochemical properties and digestibility. Both the aroid starch had low amylose content and small granule size with an A-type crystalline structure. There is no significant variation in the crystallinity percentage of both the starch. The physicochemical properties of starch are greatly influenced by the amylose - amylopectin ratio which determines the food and/or non-food application of starch. The starch from both the tubers contains low amylose content which renders it suitable as a food thickening agent. The digestibility, crystallinity and amylose content of the aroid starch granules are all found to be interrelated. Further studies are required to fully elucidate the structural and functional properties of these two starches.

Declarations

Author contribution statement

AKARSHA B., KARUNYA SHETTY: Performed the experiments; Analyzed and interpreted the data; Wrote the paper.

KRISHNAKUMAR G.: Conceived and designed the experiments; Contributed reagents, materials, analysis tools or data.

Funding statement

This work was supported by Directorate of Minorities, Karnataka.

Data availability statement

Data will be made available on request.

Declaration of interests statement

The authors declare no conflict of interest.

Additional information

No additional information is available for this paper.

Acknowledgements

We are grateful to the Chairman of the Department of studies in Physics, Director of the DST PURSE, and USIC Mangalore University for providing the necessary facilities to carry out the research.

References

Abera, G., Woldeyes, B., Demash, H.D., Miyake, G.M., 2019. Comparison of physicochemical properties of indigenous Ethiopian tuber crop (*Coccinia abyssinica*) starch with commercially available potato and wheat starches. Int. J. Biol. Macromol. 140, 43–48.

Alcázar-Alay, S.C., Meireles, M.A.A., 2015. Physicochemical properties, modifications and applications of starches from different botanical sources. Food Sci. Technol. 35 (2), 215–236.

Ambigaipalan, P., Hoover, R., Donner, E., Liu, Q., Jaiswal, S., Chibbar, R., et al., 2011. Structure of faba bean, black bean and pinto bean starches at different levels of granule organization and their physicochemical properties. Food Res. Int. 44 (9), 2962–2974.

Ashwar, B.A., Gani, A., Shah, A., Masoodi, F.A., 2017. Physicochemical properties, in-vitro digestibility and structural elucidation of RS4 from rice starch. Int. J. Biol. Macromol. 105, 471–477.

Betancur, D.A., Ancona, L.A.C., Guerrero, R.I., Camelo Matos, G., Ortiz, D., 2001. Physicochemical and functional characterization of baby lima bean (*Phaseolus lunatus*) starch. Starch-Stärke 53 (5), 219–226.

Blennow, A., Hansen, M., Schulz, A., Jørgensen, K., Donald, A.M., Sanderson, J., 2003. The molecular deposition of transgenically modified starch in the starch granule as imaged by functional microscopy. J. Struct. Biol. 143 (3), 229–241.

Chandra, R.A., Hasanah, A.N., Agustina, R., 2016. Optimization of starch from Indonesian local corn with concentration variation of sodium metabisuphite and drying time. Int. J. Chem. Eng. Appl. 7 (2), 89.

Chel-Guerrero, L., Barbosa-Martín, E., Martínez-Antonio, A., González-Mondragón, E., Betancur-Ancona, D., 2016. Some physicochemical and rheological properties of starch isolated from avocado seeds. Int. J. Biol. Macromol. 86, 302–308.

Chen, L., Tian, Y., Sun, B., Cai, C., Ma, R., Jin, Z., 2018. Measurement and characterization of external oil in the fried waxy maize starch granules using ATR-FTIR and XRD. Food Chem. 242, 131–138.

De Mejia, E.G., Prisecaru, V.I., 2005. Lectins as bioactive plant proteins: a potential in cancer treatment. Crit. Rev. Food Sci. Nutr. 45, 425–445.

Deepika, V., Kumar, K.J., Anima, P., 2013a. Isolation and partial characterization of delayed releasing starches of Colocasia species from Jharkhand, India. Carbohydr. Polym. 96 (1), 253–258.

Deepika, V., Kumar, K.J., Anima, P., 2013b. Isolation and physicochemical characterization of sustained releasing starches from Dioscorea of Jharkhand. Int. J. Biol. Macromol. 55, 193–200.

Eliasson, A.C., Gudmundsson, M., 1996. Starch: Physicochemical and Functional Aspects. Food Science And Technology-New York-Marcel Dekker-, pp. 431–504.

Falade, K.O., Okafor, C.A., 2013. Physicochemical properties of five cocoyam (Colocasia esculenta and Xanthosoma sagittifolium) starches. Food Hydrocolloids 30 (1), 173–181.

Hoover, R., 2001. Composition, molecular structure, and physicochemical properties of tuber and root starches: a review. Carbohydr. Polym. 45 (3), 253–267.

Jane, J.L., 2006. Current understanding on starch granule structures. J. Appl. Glycosci. 53 (3), 205–213.

Jane, J.L., Chen, Y.Y., Lee, L.F., McPherson, A.E., Wong, K.S., Radosavljevic, M., Kasemsuwan, T., 1999. Effects of amylopectin branch chain length and amylose content on the gelatinization and pasting properties of starch. Cereal Chem. 76 (5), 629–637.

Jobling, S., 2004. Improving starch for food and industrial applications. Curr. Opin. Plant Biol. 7 (2), 210–218.

Kuttigounder, D., Lingamallu, J.R., Bhattacharya, S., 2011. Turmeric powder and starch: selected physical, physicochemical, and microstructural properties. J. Food Sci. 76 (9), C1284–C1291.

Kouser, S., Sheik, S., Nagaraja, G.K., Prabhu, A., Prashantha, K., D'souza, J.N., et al., 2020. Functionalization of halloysite nanotube with chitosan reinforced poly (vinyl alcohol) nanocomposites for potential biomedical applications. Int. J. Biol. Macromol. 165, 1079–1092.

Lertphanich, S., Wansuksri, R., Tran, T., Da, G., Nga, L.H., Dufour, D., et al., 2013. Comparative study on physicochemical properties of ensete and water caltrop with other root, tuber, and legume starches. Starch-Stärke 65 (11-12), 1038–1050.

Liu, J., Wang, X., Bai, R., Zhang, N., Kan, J., Jin, C., 2018. Synthesis, characterization, and antioxidant activity of caffeic-acid-grafted corn starch. Starch-Stärke 70 (1-2), 1700141.

Lobo, S.M., Gulimane, K., 2015. Nutritional analysis of rhizome tuber and physicochemical characteristics of starch extracted from the mangrove fern Acrostichum aureum L. Starch-Stärke 67 (7-8), 716–719.

Lodha, G.K., Nemade, C.T., 2012. Isolation of Alocasia indica Linn. starch and its performance as a disintegrating agent. Int. J. Pharma Bio Sci. 3 (4).

Malumba, P., Doran, L., Zanmenou, W., Odjo, S., Katanga, J., Blecker, C., Béra, F., 2017. Morphological, structural and functional properties of starch granules extracted from the tubers and seeds of Sphenostylis stenocarpa. Carbohydr. Polym. 178, 286–294.

Ochubiojo, E.M., Rodrigues, A., 2012. Starch: from food to medicine. In: Scientific, Health and Social Aspects of the Food Industry, pp. 355–380.
Padmanabhan, S., Lonsane, B.K., 1992. Comparative physico-chemical and functional properties of cassava starches obtained by conventional and enzyme-integrated conventional techniques. Starch-Stärke 44 (9), 328–331.
Pascoal, A.M., Di-Medeiros, M.C.B., Batista, K.A., Leles, M.I.G., Lião, L.M., Fernandes, K.F., 2013. Extraction and chemical characterization of starch from S. lycocarpum fruits. Carbohydr. Polym. 98 (2), 1304–1310.
Perera, C., Hoover, R., 1999. Influence of hydroxypropylation on retrogradation properties of native, defatted and heat-moisture treated potato starches. Food Chem. 64 (3), 361–375.
Pfister, B., Zeeman, S.C., 2016. Formation of starch in plant cells. Cell. Mol. Life Sci. 73 (14), 2781–2807.
Riley, C.K., Wheatley, A.O., Hassan, I., Ahmad, M.H., Morrison, E.Y.S.A., Asemota, H.N., 2004. In vitro digestibility of raw starches extracted from five yam (Dioscorea spp.) species grown in Jamaica. Starch-Stärke 56 (2), 69–73.
Sadashivam, S., Manickam, A., 2008. Biochemical Methods, third ed. New AGE International (P)LTD., New Delhi, India.
Saikia, J.P., Konwar, B.K., 2012. Physicochemical properties of starch from aroids of North East India. Int. J. Food Prop. 15 (6), 1247–1261.
Sukhija, S., Singh, S., Riar, C.S., 2016. Effect of oxidation, cross-linking and dual modification on physicochemical, crystallinity, morphological, pasting and thermal characteristics of elephant foot yam (Amorphophallus paeoniifolius) starch. Food Hydrocolloids 55, 56–64.
Selvakumari, P.A.S., 2014. Pharmacognostical standardisation of *Lagenandra toxicaria* Dalz. Malays. J. Sci. 33, 163–175.
Singh, N., Singh, J., Kaur, L., Sodhi, N.S., Gill, B.S., 2003. Morphological, thermal and rheological properties of starches from different botanical sources. Food Chem. 81 (2), 219–231.
Singh, J., Colussi, R., McCarthy, O.J., Kaur, L., 2016. Potato starch and its modification. In: Advances in Potato Chemistry and Technology. Academic Press, pp. 195–247.
Singh, J., Kaur, L., McCarthy, O.J., 2007. Factors influencing the physico-chemical, morphological, thermal and rheological properties of some chemically modified starches for food applications—a review. Food Hydrocolloids 21 (1), 1–22.
Ubalua, A., 2007. Cassava wastes treatment options and values addition alternatives. Afr. J. Biotechnol. 6 (18), 2065–2073.
Van, E.D., Goossens, K., Smeets, K., Van, F.L., Verhaert, P., Peumans, W.J., 1995. The major tuber storage protein of araceae species is a lectin. Characterization and molecular cloning of the lectin from *Arum maculatum* L. Plant Physiol. 107, 1147–1158.
Wang, J., Guo, K., Fan, X., Feng, G., Wei, C., 2018. Physicochemical properties of C-type starch from root tuber of Apios fortunei in comparison with maize, potato, and pea starches. Molecules 23 (9), 2132.
Wang, J., Hu, P., Chen, Z., Liu, Q., Wei, C., 2017. Progress in high-amylose cereal crops through inactivation of starch branching enzymes. Front. Plant Sci. 8, 469.
Wani, A.A., Wani, I.A., Hussain, P.R., Gani, A., Wani, T.A., Masoodi, F.A., 2015. Physicochemical properties of native and γ-irradiated wild arrowhead (Sagittaria sagittifolia L.) tuber starch. Int. J. Biol. Macromol. 77, 360–368.
Xia, W., Wang, F., Li, J., Wei, X., Fu, T., Cui, L.,., Liu, Y., 2015. Effect of high speed jet on the physical properties of tapioca starch. Food Hydrocolloids 49, 35–41.
Yang, W., Kong, X., Zheng, Y., Sun, W., Chen, S., Liu, D., et al., 2019. Controlled ultrasound treatments modify the morphology and physical properties of rice starch rather than the fine structure. Ultrason. Sonochem. 59, 104709.
Zeng, F.K., Liu, H., Liu, G., 2014. Physicochemical properties of starch extracted from *Colocasia esculenta* (L.) Schott (Bun-long taro) grown in Hunan, China. Starch-Stärke 66 (1-2), 142–148.
Zhang, B., Guo, K., Lin, L., Wei, C., 2018. Comparison of structural and functional properties of starches from the rhizome tuber and Bulbil of Chinese Yam (*Dioscorea opposita* Thunb.). Molecules 23 (2), 427.
Zhang, L., Li, G., Wang, S., Yao, W., Zhu, F., 2017. Physicochemical properties of maca starch. Food Chem. 218, 56–63.
Zhang, S., Zhong, G., Liu, B., Wang, B., 2011. Physicochemical and functional properties of fern rhizome tuber (*Pteridium aquilinum*) starch. Starch-Stärke 63 (8), 468–474.
Zhu, F., 2016. Structure, properties, and applications of aroid starch. Food Hydrocolloids 52, 378–392.
Zhu, X., Cui, W., Zhang, E., Sheng, J., Yu, X., Xiong, F., 2018. Morphological and physicochemical properties of starches isolated from three taro bulbs. Starch Stärke 70 (1-2), 1700168.